Available online at www.sciencedirect.com

ScienceDirect

Procedia Computer Science 123 (2018) 86–91

Procedia Computer Science

www.elsevier.com/locate/procedia

8th Annual International Conference on Biologically Inspired Cognitive Architectures, BICA 2017

Neural Network Prediction of Daily Relativistic Electrons Fluence in the Outer Radiation Belt of the Earth: Selection of Delay Embedding Method*

Roman Batusov[1,2], Sergey Dolenko[1], and Irina Myagkova[1]

[1]*D.V.Skobeltsyn Institute of Nuclear Physics, M.V.Lomonosov Moscow State University, Moscow, Russia*

[2]*Physics Department, M.V.Lomonosov Moscow State University, Moscow, Russia*

dolenko@sinp.msu.ru, irina@srd.sinp.msu.ru

Abstract

Prediction of the time series of relativistic electrons fluence in the outer radiation belt of the Earth encounters problems caused by complexity and non-linearity of the "solar wind – the Earth's magnetosphere" system. Artificial neural networks are a biologically inspired architecture that is a suitable tool to solve problems of such type. This study considers the dependence of the quality of prediction on the type and depth of delay embedding of input features.

Peer-review under responsibility of the scientific committee of the 8th Annual International Conference on Biologically Inspired Cognitive Architectures

Keywords: delay embedding, time series, prediction, neural network, multi-layer perceptron, relativistic electrons of the outer radiation belt of the Earth

1 Introduction

Relativistic electrons flux of the Outer Radiation Belt of the Earth is one of the main factors of space weather since they may be harmful for spacecraft operations (e.g. (Cole, 2005), (Iucci, et al., 2005) and references there). The Earth's Radiation Belts (ERB) are the part of the Earth's magnetosphere, and they determine the radiation environment in the near-Earth space. The radiation environment at geosynchronous orbit (about 35 thousand km altitude – the outer boundary of the radiation belts) is of particular interest due to the large number of satellites populating this region. Relativistic electrons of the outer ERB are called "killer electrons" since the electronic components of spacecraft can be damaged, resulting in temporary or even complete loss of spacecraft (Dorman, et al., 2005).

* This study has been conducted at the expense of Russian Science Foundation, grant no. 16-17-00098.

Peer-review under responsibility of the scientific committee of the 8th Annual International Conference on Biologically Inspired Cognitive Architectures

10.1016/j.procs.2018.01.014

In the paper (Baker, et al., 1990) it has been found that integral day values of the fluxes – daily fluences of electrons with energy >2 MeV, measured at geosynchronous orbit, could be predicted one day ahead, using a linear filter with solar wind speed at the input. Later on, during elaboration of REFM (Relativistic Electron Forecast Model), this method was developed further for the purpose of increasing prediction quality and horizon. Prediction carried out with the help of REFM is presented at the portal (Space Weather Prediction Center, n.d.). Experimental values of electron fluence, which the prediction is compared to, are obtained in the experiment at spacecraft of GOES (Geostationary Operational Environmental Satellite) series, which were designed for monitoring of the environment (National Oceanic and Atmospheric Administration, n.d.).

An alternative approach to prediction of relativistic electron fluence in the outer ERB is based on use of artificial neural networks (ANN). This approach is used in the models presented in (Koons & Gorney, 1990) (Fukata, et al., 2002) (Ling, et al., 2010) to predict RE fluence at geostationary orbit. The authors of this study also have experience on predicting electron flux on geostationary orbit, both for hourly flux values (Myagkova, et al., 2015), (Efitorov, et al., 2016), (Myagkova, et al., 2016) and for daily fluences (Efitorov, et al., 2016).

It should be noted that the outer ERB is a complex dynamic system, it depends on the condition of the interplanetary environment – on solar wind (SW) velocity, on the values of components of the interplanetary magnetic field (IMF), geomagnetic disturbances etc. The processes in the outer ERB most likely have relaxation and nonlinear character. It leads to the fact that outer ERB has “memory”, i.e. that its instant state is not completely determined by instant values of external parameters, and the duration of the “memory” and relaxation processes for radiation belts can change. This gives us ground for a more detailed research of how far back in time values should be taken into account for prediction of daily electron fluences in the outer ERB.

2 Data Sources and Preparation

As input data for making predictions of daily fluences of relativistic (E>2 MeV) electrons at geostationary orbit, we used time series of daily aggregated values of the following physical quantities:

- SW parameters in Lagrange point L1 between the Earth and the Sun: SW speed v (measured in km/s), SW protons density n_p (measured in cm^{-3}) and SW temperature (measured in K)
- IMF vector parameters in same point L1 (measured in nT): Bx, By, Bz (IMF components in GSM system) and B amplitude (IMF modulus)
- Geomagnetic indexes: equatorial index Dst (measured in nT) and global geo-magnetic index Kp (dimensionless)
- Average daily fluence of relativistic electrons with energies >2 MeV at geostationary orbit (measured in $(cm^2 \cdot s \cdot sr)^{-1}$).

The source of the data on the SW and IMF parameters were the measurements performed continuously onboard the Advanced Composition Explorer (ACE) spacecraft (ACE Project Team, n.d.). The data on geomagnetic indexes was obtained from (World Data Center for Geomagnetism, n.d.), which provides official data for the values of geomagnetic indices, used worldwide for scientific research and practical applications. The data on relativistic electron flux was obtained from GOES project (NOAA National Centers for Environmental Information, n.d.).

Each variable was initially measured with a smaller time period, so, before being used, the data was aggregated to give time series with daily step, by averaging and/or by calculating daily minimum and maximum values of some variables (chosen based on physical considerations). Now, SW parameters and electron fluence have a wide dynamical range (more than 6 orders of magnitude), so instead of the real values of these variables, their logarithmic values were used. Also, to account for yearly

variations of the predicted quantity, sine and cosine values with yearly period were also used as input data Total number of physically different input variables of the problem was 29.

Unfortunately, data streams obtained onboard spacecraft usually have gaps. The gaps in the data shorter than 24 hours disappeared after aggregation. If they were 24 hours or longer, the corresponding patterns, containing missing data, were removed.

The whole range of data used in this study was from November 1997 (start of continuous operation of ACE spacecraft) till February 2017. The range from November 1997 till the end of 2009 (approximately one full solar activity cycle) was used as the training sample to train the ANN. The remaining period form 2010 was used as an independent test set to evaluate performance of the obtained models.

3 Description of the Numerical Experiments

To take into account the preceding states of the studied dynamical system "Sun – solar wind – Earth's magnetosphere", delay embedding was performed, i.e. each pattern was expanded with several preceding values of input variables; the maximum delay between the current moment and the moments of added values is called embedding depth. In this study, delay embedding was performed in two ways. In the first case, delay embedding of all the input variables was equal ("rectangular" embedding). Models with embedding depth of 0, 1, 2, 3, 4, 5, 10 days were investigated (0 days embedding depth means that only the current values were used). Accordingly, the model with 4 days embedding depth has 5 times as many inputs as the 0 days depth model. Deeper embedding gives the network more information to learn; on the other hand, it increases the number of weight coefficients of the ANN, increasing the danger of falling into local minima during ANN training. So, optimal embedding depth is usually determined by trial and error.

In the second case, the selection of the delays used for each variable was based on cross-correlation values between the predicted value and the values of all the input variables with various delays from 0 to 31 days. After that, only those variables whose cross-correlation coefficient was greater than some definite threshold were selected. We used two values of the threshold: 0.146, equal to the critical value of correlation coefficient for one-tailed criterion at 0.001 significance level for a large number of patterns (Fisher & Frank, 1963), and 0.368 ($1/e$).

Of course, for each variable the resulting embedding depth turned out to be different. For most of the variables, it was not greater than 2 days. Also, it was not continuous – a surge of cross-correlation values was observed on 24-26 days delay, corresponding to the period of rotation of the Sun. The total number of inputs was 318 for the value of cross-correlation coefficient threshold equal to 0.146, and 87 variables for the threshold equal to 0.368.

The ANN architecture used in the present study was the multi-layer perceptron (MLP) with a single hidden layer. The size of the hidden layer was 16 neurons, with *tanh* activation function, trained by stochastic gradient descent, with learning rate 0.001 and moment 0.5.

In total, 9 types of networks were compared: 7 types with "rectangular" embedding: ANN-0,1,2,3,4,5,10 (using the corresponding depth of embedding in days) and two types with embedding defined by the cross-correlation coefficient threshold values: ANN-CC-L and ANN-CC-H (corresponding to the lower and higher values of cross-correlation coefficient threshold).

In each experiment, 10 MLPs were trained, differing only by weights initialization. After that, the responses of the 10 networks were averaged.

The prediction has been performed with four values of the prediction horizon from 1 to 4 days ahead. Thus, 40 ANNs were trained for each of the 9 types of delay embedding.

All the obtained results are compared with each other, as well as with the results provided by the simplest trivial models, for which the prediction is equal to the last known value. Such comparison is necessary due to the fact that the changes in the predicted time series are relatively slow; therefore, even the trivial models give results with relatively high values of statistical indicators.

4 Results and Discussion

To assess the results of prediction, two statistical indicators are used in this study: the multiple determination coefficient R squared (R^2) and the root means squared error (RMSE). R^2 is dimensionless; RMSE has the same dimension as the predicted value itself, $\lg((cm^2 \cdot s \cdot sr)^{-1})$.

Table 1 shows the values of R^2 coefficient obtained on the test data set for all ANN models with various types of delay embedding, and for trivial models. Table 2 shows the values of RMSE.

Table 1. R squared values for ANN models with various types of delay embedding and for trivial models, for prediction with horizon from 1 to 4 days. Results obtained on test set.

Model \ Horizon, days	1	2	3	4
ANN-0	0,883	0,757	0,640	0,513
ANN-1	0,894	0,755	0,633	0,500
ANN-2	0,890	0,751	0,631	0,490
ANN-3	0,891	0,754	0,630	0,493
ANN-4	0,891	0,750	0,629	0,487
ANN-5	0,888	0,750	0,624	0,485
ANN-10	0,876	0,739	0,623	0,495
ANN-CC_L	0,869	0,730	0,611	0,503
ANN-CC_H	0,888	0,757	0,656	0,542
Trivial model	0,788	0,587	0,440	0,340

Table 2. RMSE values in $\lg((cm^2 \cdot s \cdot sr)^{-1})$ for ANN models with various types of delay embedding and for trivial models, for prediction with horizon from 1 to 4 days. Results obtained on test set.

Model \ Horizon, days	1	2	3	4
ANN-0	0,377	0,548	0,671	0,777
ANN-1	0,360	0,550	0,675	0,787
ANN-2	0,365	0,552	0,675	0,793
ANN-3	0,365	0,549	0,676	0,791
ANN-4	0,365	0,555	0,677	0,794
ANN-5	0,369	0,556	0,681	0,795
ANN-10	0,383	0,558	0,670	0,773
ANN-CC_L	0,371	0,534	0,639	0,726
ANN-CC_H	0,362	0,538	0,643	0,739
Trivial model	0,521	0,752	0,903	1,005

To make the results more demonstrative, Figure 1 presents the difference between R squared values of each ANN model and that of the corresponding trivial model with the same prediction horizon. Figure 2 presents the difference between the RMSE values of the trivial models and those of each ANN model with the same prediction horizon.

From analysis of the Tables and Figures, the following conclusions can be made.

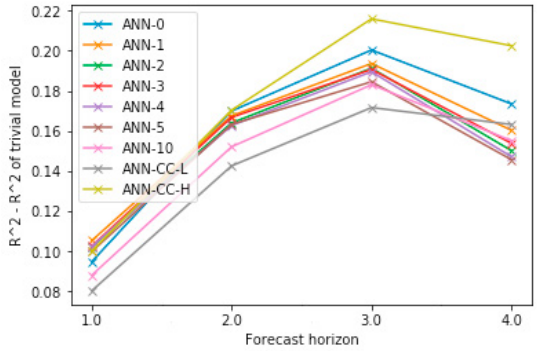

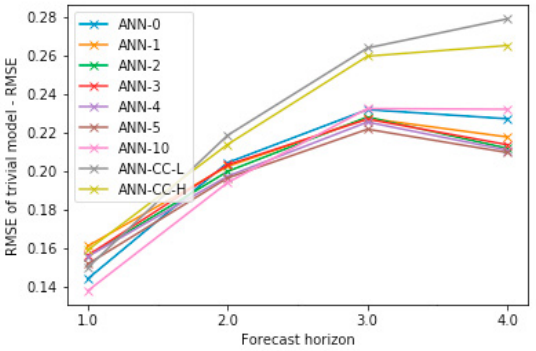

Figure 1 (left). Difference between R squared values of each ANN model and that of the corresponding trivial model with the same prediction horizon.

Figure 2 (right). Difference between the RMSE values of the trivial models and those of each ANN model with the same prediction horizon.

1) Increase in the embedding depth for "rectangular" embedding provides additional information for the ANN, but increases the number of ANN weights, thus increasing the danger of falling into local minima during ANN training. So optimal value of the depth of "rectangular" delay embedding is different for different cases, e.g. for different values of the prediction horizon.

2) Selection of the necessary delays based on CC values provides a more informative set of inputs for the ANN, as the most informative delays for various physical quantities may be different. In particular, taking into account the data for one solar rotation back allows improving the quality of the prediction. Selection of the CC threshold for selection of the delays may be a subject of a separate study. In this study, use of a lower threshold, equal to the critical value of correlation coefficient for one-tailed criterion at 0.001 significance level for a large number of patterns, provided better results.

3) Different statistical indexes used to assess the prediction quality are not equivalent, so several indexes should be used simultaneously to select the optimal configuration of the predicting system.

4) The obtained results differ for different values of the prediction horizon. While all the models obviously degrade with prediction horizon, the quantitative measures of this degradation vary. In the considered range of prediction horizons, the highest advantage of ANN models is achieved for the predictions three days ahead.

5) The results for prediction horizon of 1 day are different from those for predictions with longer horizons. This may be due to the fact of availability of data for the day just preceding the day for which the prediction is made, bearing the largest amount of necessary information among all the possible inputs of a model.

6) In general, the degradation of all the models with prediction horizon is not very rapid. Therefore, future studies should include experiments on further increase of the prediction horizon.

5 Conclusion

This paper presents the results of investigation of the influence of the method of delay embedding on the results of prediction of the daily fluence of relativistic electrons in the outer radiation belt of the Earth by perceptron type artificial neural networks. It has been demonstrated, that use of "rectangular" embedding (equal embedding depth for all the physical quantities and a continuous set of embedding delays from 0 to the selected depth) is not very efficient. The best results have been shown by selection of the necessary delays based on the values of cross-correlation coefficient with the predicted values. Future studies should be aimed at developing a more sophisticated selection procedure taking into account non-linear dependencies in the data.

References

ACE Project Team, n.d. *Advanced Composition Explorer (ACE) Home Page.* [Online]
Available at: http://www.srl.caltech.edu/ACE/
[Accessed 19 July 2017].

Baker, D., McPherron, R., Cayton, T. & Klebesadel, R., 1990. Linear prediction filter analysis of relativistic electron properties at 6.6 RE. *J. Geophys. Res.,* 95(A9), pp. 15133-15140.

Cole, D., 2005. Space weather: Its effects and predictability. *Space Science Reviews,* Volume 107, pp. 295-302.

Dorman, L., Iucci, N. & Belov, A. e. a., 2005. Space weather and space-crafts anomalies. *Annales Geophys.,* 23(9), pp. 3009-3018.

Efitorov, A., Myagkova, I. & Dolenko, S., 2016. *Prediction of maximum daily relativistic electron flux at geostationary orbit by adaptive methods.* [Online]
Available at: http://geo.phys.spbu.ru/materials_of_a_conference_2016/STP/27_Efitorov.pdf
[Accessed 4 July 2017].

Efitorov, A. et al., 2016. Prediction of Relativistic Electrons Flux in the Outer Radiation Belt of the Earth Using Adaptive Methods. *Advances in Intelligent Systems and Computing,* Volume 449, pp. 281-287.

Fisher, R. & Frank, Y. eds., 1963. *Statistical Tables for Biological, Agricultural and Medical Research.* 6th ed. ed. London: Longman Group, Ltd..

Fukata, M., Taguchi, S., Okuzawa, T. & Obara, T., 2002. Neural network prediction of relativistic electrons at geosynchronous orbit during the storm recovery phase: effects of recurring substorms. *Ann. Geophys.,* 20(7), pp. 947-951.

Iucci, N., Levitin, A. & Belov, A. e. a., 2005. Space weather conditions and spacecraft anomalies in dfferent orbits. *Space Weather,* 3(1), p. S01001.

Koons, H. & Gorney, D., 1990. A neural network model of the relativistic electron flux at geosynchronous orbit. *J. Geophys. Res.,* Volume 96, p. 5549–5556.

Ling, A., Ginet, G., Hilmer, R. & Perry, K., 2010. A neural network-based geosynchronous relativistic electron flux forecasting model. *Adv. Space Res. (Space Weather),* 8(9), p. S09003.

Myagkova, I. et al., 2015. Horizon of Neural Network Prediction of Relativistic Electrons Flux in the Outer Radiation Belt of the Earth. *ACM Proceedings*, p. article no.9.

Myagkova, I., Shiroky, V. & Dolenko, S., 2016. Effect of Simultaneous Time Series Prediction with Various Horizons on Prediction Quality at the Example of Electron Flux in the Outer Radiation Belt of the Earth. *Lecture Notes in Computer Science,* Volume 9887, pp. 317-325.

National Oceanic and Atmospheric Administration, n.d. *GOES Space Environment Monitor - Data Access.* [Online]
Available at: https://www.ngdc.noaa.gov/stp/satellite/goes/dataaccess.html
[Accessed 4 July 2017].

NOAA National Centers for Environmental Information, n.d. *GOES Space Environment Monitor.* [Online]
Available at: https://www.ngdc.noaa.gov/stp/satellite/goes/index.html
[Accessed 19 July 2017].

Space Weather Prediction Center, n.d. *Relativistic Elecron Forecast Model.* [Online]
Available at: http://www.swpc.noaa.gov/products/relativistic-electron-forecast-model
[Accessed 4 July 2017].

World Data Center for Geomagnetism, n.d. *Geomagnetic Data Service in Kyoto.* [Online]
Available at: http://wdc.kugi.kyoto-u.ac.jp/wdc/Sec3.html
[Accessed 19 July 2017].